Seasonal characteristics of the relationship between daily precipitation intensity and surface temperature

P. Berg,[1] J. O. Haerter,[2] P. Thejll,[3] C. Piani,[4] S. Hagemann,[2] and J. H. Christensen[3]

Received 5 March 2009; revised 26 June 2009; accepted 2 July 2009; published 16 September 2009.

[1] Past studies have argued that the intensity of extreme precipitation events should increase exponentially with temperature. This argument is based on the principle that the atmospheric moisture holding capacity increases according to the Clausius-Clapeyron equation and on the expectation that precipitation formation should follow accordingly. We test the latter assumption by investigating to what extent a relation with temperature can be observed intraseasonally in present-day climate. For this purpose, we use observed and simulated daily surface temperature and precipitation over Europe. In winter a general increase in precipitation intensity is indeed observed, while in summer we find a decrease in precipitation intensity with increasing temperature. We interpret these findings by making use of model results where we can distinguish separate precipitation types and investigate the moisture content in the atmosphere. In winter, the Clausius-Clapeyron relationship sets a limit to the increase in the large-scale precipitation with increasing temperature. Conversely, in summer the availability of moisture, and not the atmosphere's capacity to hold this moisture, is the dominant factor at the daily timescale. For convective precipitation, we find a peak like structure which is similar for all subregions, independent of the mean temperature, contrary to large-scale precipitation which has a more monotonic dependence on temperature.

Citation: Berg, P., J. O. Haerter, P. Thejll, C. Piani, S. Hagemann, and J. H. Christensen (2009), Seasonal characteristics of the relationship between daily precipitation intensity and surface temperature, *J. Geophys. Res.*, *114*, D18102, doi:10.1029/2009JD012008.

1. Introduction

[2] What is the connection between precipitation intensity and the surface temperature? A claim commonly made when studying global warming is that precipitation intensity increases as the troposphere warms [*Hennessy et al.*, 1997; *Allen and Ingram*, 2002; *Semenov and Bengtsson*, 2002; *Trenberth et al.*, 2003]. This claim has its origin in the relationship between the air's moisture-holding capacity and the temperature, as stated by the Clausius-Clapeyron (C-C) equation. This equation gives roughly a 7% increase in atmospheric moisture storage potential per degree Kelvin [*Trenberth et al.*, 2003].

[3] In a recent study of the De Bilt precipitation station in the Netherlands [*Lenderink and van Meijgaard*, 2008], the relationship between the intensity of extreme precipitation and surface temperature for hourly and daily values was studied. An exponential increase following the C-C equation for low to intermediate temperatures was found for both daily and hourly precipitation intensities. Furthermore, for the hourly resolved precipitation a "super C-C" relation (i.e., an increase at a rate higher than $7\%K^{-1}$) was identified at the higher range of temperatures. While this study made a serious attempt in understanding the statistical relation between those two quantities on a short timescale, the distinction between the response in different seasons was not shown. This obscures the role of the different mechanisms contributing in summer and winter to the European climate as the statistical distribution includes data from all seasons. For instance, the relative contributions of synoptic weather systems, that are dominant in winter in northern Europe, and local thunderstorm-like events, prevalent in summer, has not been distinguished. It has furthermore been argued that the "super-C-C" relation found could be an artifact of the timescale studied causing an apparent increase at hourly timescales [*Haerter and Berg*, 2009]. We advocate the approach of distinguishing seasons to allow a more detailed investigation of the mechanisms responsible for the precipitation increase.

[4] Several studies explore the trends in heavy precipitation intensities in a global warming scenario. In the observational record, an increase in heavy and very heavy precipitation intensities over the 20th century has been reported for several regions of the world [*Groisman et al.*, 2005]. A major part of the available scenario simulations of future climate, using general circulation models (GCMs) and regional climate models (RCMs), shows an increase in the heavier precipitation intensity at the cost of decreasing

[1]Water Cycle and Climate Modeling, Institute for Meteorology and Climate Research, University of Karlsruhe and Karlsruhe Forschungszentrum, Karlsruhe, Germany.
[2]Land in the Earth-System, Max-Planck-Institute for Meteorology, Hamburg, Germany.
[3]Danish Climate Centre, Danish Meteorological Institute, Copenhagen, Denmark.
[4]International Center for Theoretical Physics, Trieste, Italy.

0148-0227/09/2009JD012008

lighter precipitation [*Hennessy et al.*, 1997; *Meehl et al.*, 1999; *Semenov and Bengtsson*, 2002; *Allen and Ingram*, 2002; *Meehl et al.*, 2005; *Sun et al.*, 2007; *Gutowski et al.*, 2007; *Boberg et al.*, 2008]. The agreement between the models and the observations gives confidence to seeking explanations for the increase in extreme precipitation in basic physical processes which are included in the models. Possible processes leading to the increase in extreme precipitation intensities can be changes in the atmospheric circulation [*Emori and Brown*, 2005]; changes in the large scale distribution of atmospheric aerosols, and their effect on the distribution of energy in the troposphere and on the surface; or through an intensification and invigoration of the cloud and precipitation formation process [*Allen and Ingram*, 2002]. For the latter of these processes, it has been argued that a rise in surface temperature will enhance the intensity of heavy precipitation events through an increase in atmospheric moisture, which is fed to a precipitation event through low-level moisture convergence [*Trenberth et al.*, 2003]. The hypothesis is that precipitation intensity would then follow the increase in atmospheric moisture.

[5] Whether or not an increase in the surface temperature leads to an increase in heavy precipitation depends on several factors: the moisture holding capacity of the atmosphere, the atmospheric circulation and its vertical temperature profile, as well as microscale processes that might come into play [*IPCC*, 2007; *Dai*, 2006; *Trenberth et al.*, 2005]. For large-scale systems, the water availability is of further importance. These are all factors that change with the seasons. The general relationship between monthly mean surface temperature and total monthly precipitation amount has been studied globally, showing positive correlations over land in winter when the moisture holding capacity of the atmosphere is low, and negative correlations in summer [*Trenberth and Shea*, 2005]. The negative correlations were argued to be caused by dry conditions favoring more sunshine, and less evaporative cooling, while wet conditions occur predominantly in cool summers. Their study addressed the seasonal changes in the dependence of total monthly precipitation on surface temperature. However, the use of monthly mean values prevents a separation between times with and without precipitation, which makes the results difficult to assess with respect to precipitation intensity. To test a hypothesis about the precipitation intensity, which fluctuates on timescales much shorter than months, a study of daily precipitation data is a step forward, even though an even higher temporal resolution is desirable.

[6] In the present work we study the intraseasonal relationship between temperature and precipitation intensity, building further upon the work by *Lenderink and van Meijgaard* [2008]. To this end we use a gridded observational data set of daily values covering all of Europe. We investigate where and in which seasons the precipitation intensity dependence on temperature can be related to the C-C relation, and why this concept breaks down in other regions or seasons. The results are compared to, and further explored with, RCM simulations of the same present-day period. The data sets and models used are presented in section 2. Section 3 contains a discussion on the study region and its characteristics. The method and the significance tests used are explained in section 4. The results section is subdivided into observational aspects, section 5, and a model part, section 6. We end with summary and conclusions in section 7.

2. Data and Models

[7] We use a gridded 0.44 degree resolution observational data set of daily precipitation and temperature over European land areas [*Haylock et al.*, 2008], constructed for the ENSEMBLES project [*Hewitt and Griggs*, 2004]. Our focus is on the period 1961–1990, where there is good spatial and temporal coverage of precipitation and temperature stations in the domain. As a sanity check, we have also analyzed the parts of the station data underlying the gridded data set, which are available from the ECA&D [*Tank et al.*, 2002] data set, to assess differences in the precipitation intensities between the two data sets. The gridded data set reproduces the statistics derived from the station data to the precision required for this study. Furthermore, the station data were also used for comparison in the following study, yielding consistent results (not shown) with what we find for the gridded data in section 5.

[8] To complement the observations we use ERA40 reanalysis driven simulations by the HIRHAM4 [*Christensen et al.*, 1996], REMO [*Jacob et al.*, 2001], and HadRM3 [*Collins et al.*, 2006] RCMs from the ENSEMBLES project. To be consistent with the observational data set, we use only model data over land. Earlier versions of these models have been shown [*Boberg et al.*, 2008] to represent a good cross-section of the range of results produced by the PRUDENCE project [*Christensen and Christensen*, 2007]. All three models have a horizontal resolution of 0.44 degrees, and 19 vertical levels for HIRHAM and HadRM, while REMO has 27. The HIRHAM and REMO models are both based on the physical parameterization package of the ECHAM4 general circulation model. Thus they have the same numerical schemes for large scale, P_{ls} [*Lohmann and Roeckner*, 1996; *Tompkins*, 2002] and convective, P_c, precipitation [*Tiedtke*, 1989; *Nordeng*, 1994] etc., although details have changed due to the independent evolution of the regional models. Also, the dynamical cores of the models differ. The HadRM model differs from the other two in having both different P_{ls} [*Senior and Mitchell*, 1993; *Gregory*, 1995] and P_c [*Gregory and Rowntree*, 1990; *Gregory and Allen*, 1991] schemes and dynamics.

[9] It is not the subject of this paper to go into details of how the schemes and parameterizations differ. Instead, our focus is on observational features that are consistently captured by all models. The output of these models provides us with a physically consistent set of meteorological quantities, which we do not have access to in the observational data. Employing regional climate model output offers crucial advantages over global climate model data, not just because of the increase in resolution, but also in that known boundary conditions (within the error bars of reanalysis data) can be specified explicitly at the lateral boundaries of the model. Thereby internally consistent fields are produced within the domain of interest. This does not equally apply to global model data, even when nudging with observational data is attempted.

3. The Study Region and Its Characteristics

[10] We study the entire European domain (EU) as well as eight subregions: the British Isles (BI), the Iberian Peninsula

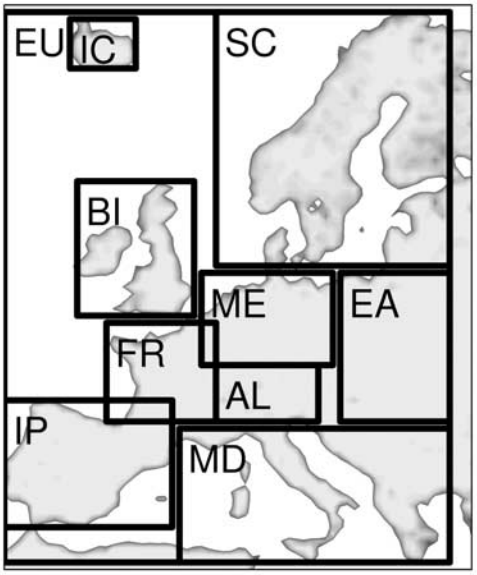

Figure 1. The European study region (EU) and its subregions BI (British Isles), IP (Iberian Peninsula), FR (France), ME (Middle Europe), SC (Scandinavia), AL (Alps), MD (Mediterranean), EA (Eastern Europe), and IC (Iceland).

(IP), France (FR), Scandinavia (SC), Middle Europe (ME), the Alps (AL), the Mediterranean (MD), Eastern Europe (EA) and Iceland (IC), based on the definitions in the work of *Christensen and Christensen* [2007] (Figure 1). The subregions are intended to break down EU in areas with distinct climatological characteristics.

[11] In winter, Europe is predominantly affected by synoptic weather systems from the Atlantic ocean, bringing mild moist air over the continent. At times, there are blocking events that disrupt the westerly flow of the atmosphere, and a north-south or south-north flow takes over. The British Isles and northern Europe are mostly influenced by the Atlantic ocean with mild winters as a consequence, while central and eastern Europe have a more continental climate, and thus colder and drier winters. The Iberian Peninsula and the Mediterranean regions have typically wet and mild winters, while the summers are hot and dry. In summer, convective precipitation events are more common, and precipitation is generally more intense in middle and southern Europe [*Landsberg*, 1970].

[12] The probability distribution function (pdf) of precipitation differs substantially among the European regions, with, e.g., low intense, but frequent precipitation in the British Isles (BI), and rare but high intensity precipitation over the Iberian Peninsula (IP). Figure 2 in the work of *Boberg et al.* [2008] shows how the intensity probability distribution function (pdf) differs among different regions of Europe, and how the RCMs of the PRUDENCE project agree to a high degree.

4. Method

[13] We consider daily precipitation intensity, P, and the two-meter daily mean temperature, T. Unless stated otherwise, in what follows we refer to average daily precipitation intensity, hence daily total amount divided by 24 hours, whenever we use the term precipitation intensity. Note that certain processes that occur on subdaily timescales, such as the diurnal cycle of precipitation, cannot be resolved by the data. Furthermore, the frequency and duration of precipitation events will likely vary between seasons. We assume here that the surface temperature stands in a well-defined relationship to cloud level temperature, which is the relevant quantity for the atmospheric moisture holding capacity at cloud level. This is found to be valid for the RCMs in this study on a daily timescale (not shown). Our assumption holds as long as the temperature lapse rate of the lower atmosphere does not change significantly. An analysis on subdaily timescales would be required to further address the validity of this assumption.

[14] In a first step we compose for each grid box (T, P) pairs of temperature and the corresponding precipitation intensity for all daily time steps with more than 0.1 mm of precipitation, i.e., only for wet days, and for all subregions. We produce separate statistics for each month of the year and for each of the subregions. Due to the different sizes of the subregions, the number of (T, P) pairs available ranges from less than 100,000 in the smallest region, IC, to about 4,000,000 in the largest region, EU. To test for a relationship between the temperature and precipitation intensity, we divide the data into bins of two Kelvin, and calculate the 70th, 90th, 99th and 99.9th percentiles. The 99th and 99.9th percentiles are calculated using a Generalized Pareto Distribution (GPD) fitted to the highest 20% of precipitation intensities. The Gamma distribution, as has earlier been extensively employed in precipitation studies [*Semenov and Bengtsson*, 2002; *Gutowski et al.*, 2007] was also tested and gave similar results. However, the goodness of fit of the Gamma distribution is not as consistent as that of the GPD, so we opted for the latter. To have a reasonable fit to the data, we require that at least 300 data points are available in each temperature bin.

[15] The goodness of fit is calculated by a Monte Carlo method of subsampling the data. A set of one hundred surrogate data sets with varying subsampling are made, and a new fit is computed for each of them. The confidence interval of the percentiles in each temperature bin can then be calculated. We find the confidence intervals to be sufficiently small so that they do not impact decisively on the results in the relationships studied in this paper.

[16] In a second test, we want to assess the significance of the trend of the percentiles, i.e., the likelihood of any trend arising by chance. This is performed with a Monte Carlo simulation where surrogate data are constructed from a bootstrap with replacement [*Efron and Tibshirani*, 1993] of the original data. The bootstrap is carried out on the precipitation time series in each grid point, so that the surrogate data sets compare precipitation from one day to the temperature of another, randomly chosen, day within the same month of the year. In this way the number of events in each temperature bin is retained, and the significance test tells us whether the intensity in the bin is significantly different from the randomly calculated intensity. The decorrelation time of the data is important for the bootstrap procedure. We find that temperature anomalies have a maximum decorrelation time (correlation less than e^{-1}) of

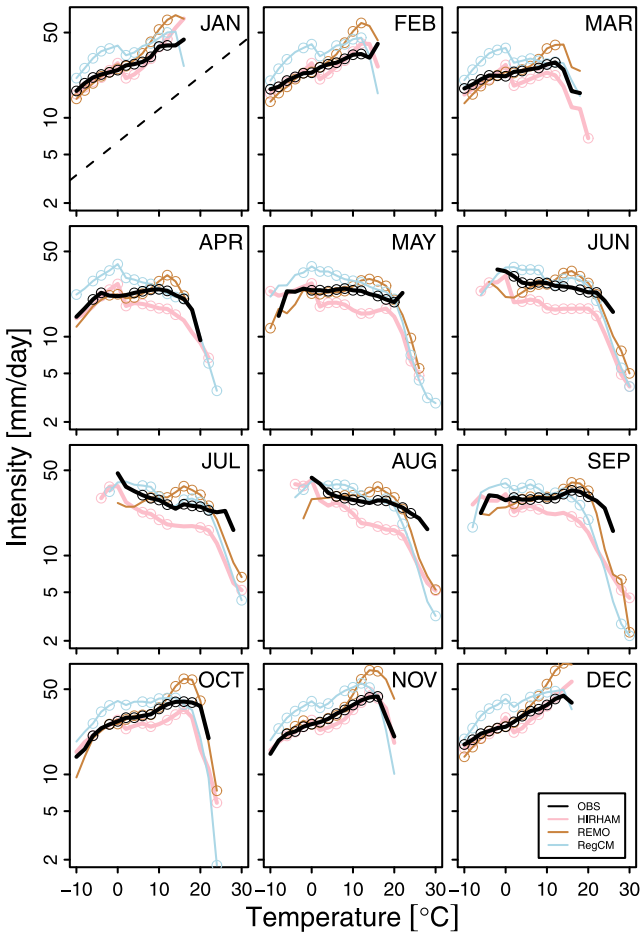

Figure 2. The 99th percentile of precipitation intensity larger than 0.1 mm d^{-1} as a function of daily average temperature for observations (black), HIRHAM4 (pink), REMO (light brown), and HadRM (light blue). The data are separated into months to show the seasonal cycle, and data points that are significant to the 95% level and has a spread of the confidence interval which is less than 10% of the value are marked with a ring. The dashed line shows a C-C like 7%/*K* increase with temperature. Note the logarithmic vertical axis.

about eight days, while precipitation anomalies have a maximum decorrelation time of about one to two days. The block size of the bootstrap is therefore set to eight days, a conservative choice. One hundred surrogate time series are found to be enough to calculate the significance. As expected, we find the percentiles of the surrogate data ensemble to have no temperature dependency, and the spread of the surrogates is on the order of a few millimeters of daily precipitation. The surrogate data are not shown in the figures, but the data points which are significantly different from the "cloud" of surrogate data to the 95% level are marked by a ring in Figure 2.

5. Results From Observations

[17] In this section we describe the observational findings for the relation between temperature and precipitation intensity, and compare to the modeled data. First we focus on the EU region, which covers all the smaller subregions. In a second step we explore whether the subregions show different behavior.

5.1. Europe

[18] For the EU region we show plots of the 99th percentile for each month computed from the observational and model data sets (Figure 2). The 70th, 90th, and 99.9th percentiles were also computed; however, these high percentile curves generally follow parallel temperature dependence, making a presentation of all percentiles redundant. For all months of the year we find a reasonable agreement between the observations and the models, both in respect to the magnitude of the intensities and the qualitative behavior.

[19] In the winter months (December to February), precipitation intensity shows a clear positive relationship with increasing temperature. The increase follows roughly that of the C-C equation which is indicated by a dashed line in the top left plot of Figure 2. All three models show a similar positive trend, even though there are variations between the models and a dip around the melting point that is likely due to model artifacts of snowmelt.

[20] In summer (June to August) there is a negative relationship between precipitation intensity and temperature, both in models and in observations. This is a feature that would not be visible if the statistics were taken over the entire year. Interestingly, the curve in summer does not show the same kind of monotonic temperature dependency as that in winter. The behavior of the summer trend is clearer in the subregions, and we will return to this topic in section 5.2 and section 6. The models again reproduce the structure of the observations, but with a more pronounced breaking of the negative summer trend with an upturn at intermediate temperatures, and also a more pronounced return to the negative trend at higher temperatures. In spring (March to May) and autumn (September to November) the behavior is transitional between that in winter and summer described above, with a general increase at low temperatures and a decrease at higher temperatures. The models and observations show a high degree of agreement in these periods.

5.2. Subregions

[21] The qualitative pattern of the larger region is generally preserved also for the subregions (Figure 3). For clarity, we focus on the observations for the months of January and July where we have the strongest trends. The model data agree generally with the observations. The southern and western subregions (IP, BI, FR, MD) are characterized by a weaker positive winter trend than the EU region, while the northern regions (SC and ME) display a much steeper trend. The IC region contains too little data to yield any significant results. In July, the southern subregions (IP, MD) yield a steep and rather strict exponential decline in summer. For the other regions (except AL), the summer curve follows a different behavior with a break in the negative trend, often showing an oscillatory behavior rather than the monotonic downward slope. The model data for these regions produce a similar pattern, but with a larger temperature range, showing the return to the negative trend at higher temperatures, as exemplified by the HIRHAM model in Figure 3.

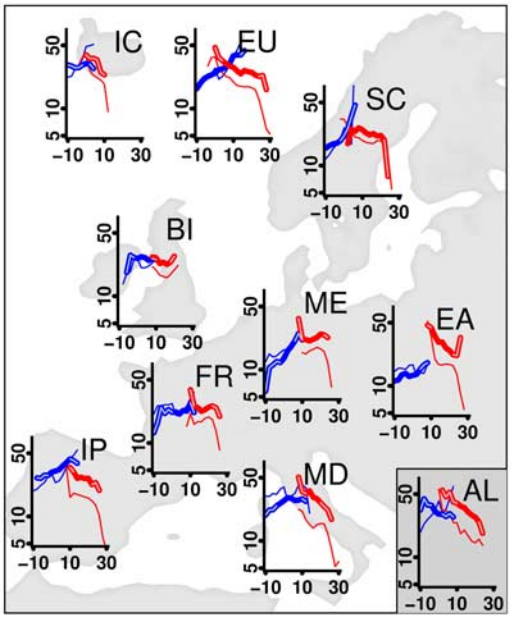

Figure 3. 99th percentile of precipitation intensity larger than 0.1 mm d^{-1} as a function of daily average temperature for observations in January (blue) and July (red) for the different subregions. The horizontal axis is temperature in degree Celsius, and the vertical is precipitation intensity in mm/day, i.e., the same as in Figure 2. Results are shown for the observations (thick lines) and for the HIRHAM model (thin lines) for comparison. Dark (light) colors in the curves indicate that the spread of the confidence interval is less (larger) than 10%. Note the logarithmic vertical axis.

The AL subregion differs from the other regions in that it shows a monotonic negative trend in both winter and summer. This behavior might be an artifact of the gridding of the station data, but we have not investigated this aspect further. This analysis of the subregions shows consistency with the features found in the EU region, but with some regional variations.

[22] The results presented here expand on the conclusions drawn from a study of a single observational station in the Netherlands, where the authors found an increase in precipitation intensity with temperature, in statistics involving the whole year without distinction of months or seasons [*Lenderink and van Meijgaard*, 2008]. Our results are consistent with theirs when statistics are taken without distinction of seasons and in a comparable subregion around De Bilt.

6. Results From RCMs

[23] As we have generally found good agreement between observations and models for all regions and months, we are encouraged to investigate the underlying mechanisms within the model output. There are some quantitative differences between the models, e.g., the percentiles from the HIRHAM model are generally lower than for the other two models. There are also differences between models and observations, e.g., at high temperatures the model percentiles between May and September fall off more quickly than in the observations (Figure 2). However, models and observations are qualitatively compatible in the way the main trends are simulated. In the following we investigate separately P_{ls} and P_c, and we analyze the data for atmospheric moisture to better understand the behavior of the observational and model precipitation percentiles as a function of temperature.

6.1. Large-Scale and Convective Precipitation

[24] To further explore the physics behind the trends identified from Figure 2, we make a distinction between P_{ls} and P_c precipitation events. P_{ls} occurs as a consequence of slow ascent of air in synoptic systems, e.g., along cold fronts, and in advance of warm fronts, while P_c is triggered by local instabilities and convective motions in the atmosphere. P_{ls} typically brings low intensity precipitation over a large area for several hours up to a day, while P_c has a more showery character with short intense events, and only affects smaller geographical regions. The distinction is made in the climate models themselves, where different numerical schemes are applied to the two precipitation types. Hence notwithstanding the somewhat artificial separation between the two precipitation types in numerical models as well as different ways of doing so between the models, we employ such model data to explore a more quantitative description of the actual precipitation statistics. Furthermore, the separation between large-scale and convective events in the models used here is mainly carried out according to the magnitude of near-surface moisture convergence, a quantity that is also of interest to our analysis since it provides a measure of the process leading to the precipitation event. This is how the separation should be understood in the following analysis.

[25] In Figure 4 the total precipitation for the HIRHAM RCM is plotted along with its large-scale and convective components. In the bottom of each plot, the relative contribution from the two precipitation schemes to the total normalized precipitation is shown. The curves for P_c and P_{ls} follow rather distinct behavior: P_c generally increases (decreases) with temperature at low (high) temperatures and displays a peak at intermediate temperatures with no qualitative seasonal dependence. P_{ls} follows an exponential increase in winter, with a coefficient close to that of the C-C relation, but a general downward slope in summer. In the transitional seasons a rather featureless behavior, perhaps resembling a superposition of the two extremes, is found. When the relative contributions of the two types of precipitation are taken into account, it becomes obvious how the curve of total precipitation can be understood as a weighted superposition of P_{ls} and P_c. P_{ls} dominates at low temperatures and in winter. While P_{ls} contributes to the total precipitation year-round, P_c gains importance only for the intermediary and high end of the temperature ranges in summer. Note that for a higher temporal resolution of the precipitation, P_c will have a larger impact on the intensities, as it is generally of a much shorter timescale than that studied here.

[26] When we focus again on the peak structure in the curves of P_c we first note that this peak defines the temperature of strongest precipitation extremes, T_{ex}, a temperature of considerable importance when, e.g., dealing with flood risk. Since the plots in Figure 2 obscure regional

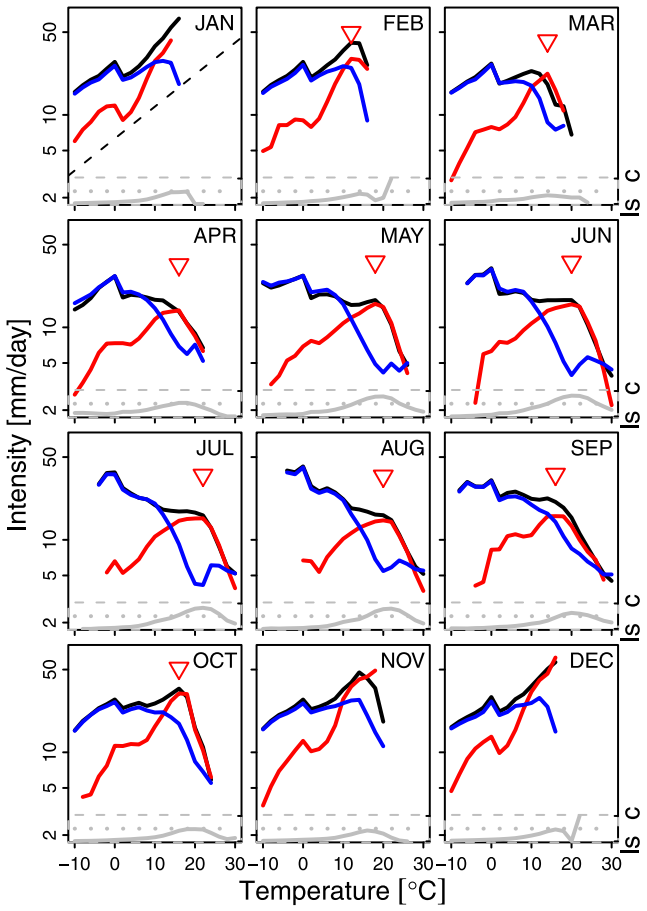

Figure 4. Similar to Figure 2, but for HIRHAM model only. The plots show total (black), large-scale (blue), and convective (red) model precipitation. The dotted line in the plot for January shows the increase by $7\%K^{-1}$ as described by the C-C relation. The red triangles mark the location of the peak temperature T_{ex} for the convective precipitation. In the bottom part of each plot the difference of the convective and large-scale contributions to the total precipitation $(P_c(T) - P_{ls}(T))/(P_c(T) + P_{ls}(T))$ are shown in a gray color: the two precipitation types contribute equally when the curve (gray) is close to the dotted line in the center of the graph, else the convective (c) or large-scale (ls) dominates. The gray curve extends beyond the other curves because the ratio of total amount can be defined in some bins where data is not sufficient for 99th percentile.

fluctuations, such as the dependence on latitude, we proceed by extracting T_{ex} from all subregions. The results are similar in all three models, and we therefore construct an ensemble mean of the results, as shown in Figure 5. All regions have a seasonal cycle of T_{ex}, with highest values in July or August and lowest values in winter. Interestingly, there is no clear difference between the values of T_{ex} in the different regions. In the comparison between SC and IP, which have the largest latitudinal difference, the T_{ex} for SC is in fact slightly higher than that for IP. This finding is surprising in the light of the strong differences in average surface temperature between these regions in summer. In summary, the appearance of the peak in convective precipitation percentiles does not seem to be a feature that varies with latitude, but rather a scale specific to the mechanism behind P_c. To test whether the feature of a negative trend above T_{ex} is due to a cooling off as a consequence of heavy precipitation events, we make use of the daily maximum temperatures. The results are very similar also when this more instantaneous variable is used, and we can reject this simplistic explanation.

6.2. Atmospheric Moisture

[27] In an effort to explain the relationships found in the above analysis, we now consider the atmospheric moisture in a similar temperature-dependent analysis. There is not much observational data available for the land regions studied here, and especially not in a climatological context. We therefore make use of daily model results to investigate the origin of the different statistical behaviors in summer and winter. Note that an investigation of convective precipitation, the diurnal cycle or moisture convergence would require the analysis of at least hourly data. Such an analysis is planned for a future study, but here we settle for the daily data at hand. Because of this, the results are biased to the behavior of P_{ls} due to its longer timescale. No specific validation has been made for the model data, due to the lack of observational data to validate with, but the similarity of the relationships presented for all three models builds confidence in the results. In the left column of Figure 6 we present plots of precipitation intensity versus daily

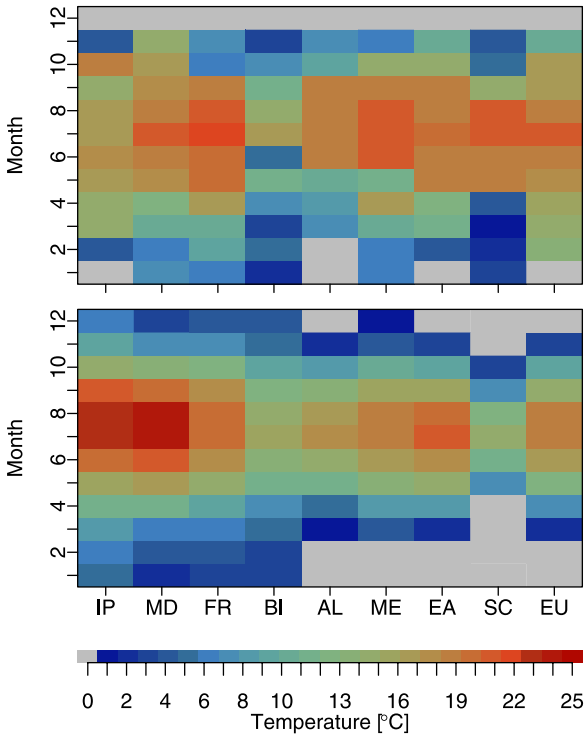

Figure 5. (top) Peak temperature T_{ex} of the 99th percentile of convective precipitation as a function of region (horizontal axis, compare Figure 1) and month (vertical axis). The plot shows an ensemble of the three RCMs, which individually yield similar results. Gray fields correspond to missing values, i.e., no peak could be defined in the data, or values below zero degrees Celsius. (bottom) The monthly mean temperature for each region and month.

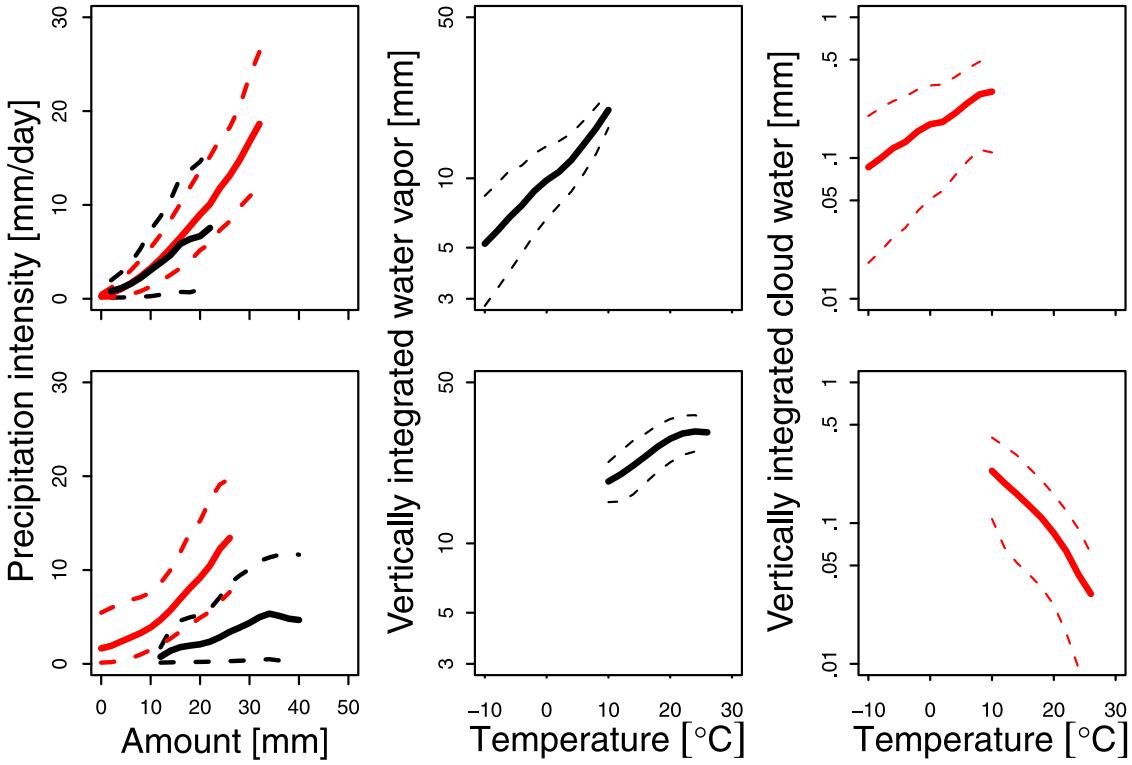

Figure 6. (left column) Curves for mean (solid) and 10th and 90th percentiles (dashed) for precipitation intensity as a function of the daily average vertically integrated water vapor (black curves) and cloud water (red curves, values of cloud water multiplied by 50 for better presentation). (middle column) Vertically integrated water vapor as a function of surface temperature. (right column) Vertically integrated cloud water as a function of surface temperature. The top row shows the results for January, and the bottom row for July, for the ME subregion. Note the logarithmic vertical scales in the middle and right columns. All plots are conditional on wet days.

average vertically integrated water vapor (q_v) and vertically integrated cloud water (q_l) for wet days ($P > 0.1$ mm/d). We show only the data obtained for the spatially fairly uniform ME region from the HIRHAM model as a typical example. Other subregions and models show comparable behavior. While there is a rather well-defined relationship between cloud water and precipitation intensity, precipitation intensity and q_v are not as clearly related, especially in summer.

[28] The relationship between q_v and surface temperature (middle column of Figure 6) shows a strictly exponential increase in winter with a coefficient that matches precisely that dictated by the C-C relation $q_v(T) \propto \exp(bT)$ with $b \approx 0.07K^{-1}$. While there is also an exponential increase in summer, the increase is much weaker with an exponent of only $b \approx 0.03K^{-1}$ (which we call *sub-C-C coefficient*). q_l shows an exponential increase with surface temperature in winter (right column) while the relation is completely reversed in summer with a strict exponential decrease.

[29] The first striking observation from this analysis is that cloud water and water vapor are linked in winter while this link is altered in summer. The second is that precipitation intensity is tied to q_l but not directly to q_v, especially in summer. The more subtle, yet basic, lesson drawn from this exercise is that cloud water is the consequence of a saturated atmosphere. In winter, due to the saturation criterion provided by the C-C relation, saturation takes place at rather low temperatures. Therefore only a relatively small supply of water vapor is required to yield saturation and consequently condensation of cloud droplets. In summer, larger quantities of atmospheric moisture are required to drive the atmosphere to saturation. The sub-C-C coefficient b in summer implies that q_v increases more slowly than demanded for saturation by the C-C relation. This means that it becomes less likely to find saturation, and hence condensation, in the atmosphere with further increasing temperatures. Therefore there is a lack of q_l with increasing temperatures.

7. Summary and Conclusions

[30] We have carried out a study of both observational and model data for daily precipitation intensity and its dependence on daily mean temperature. The study is carried out using daily precipitation and temperature data from a gridded observational data set, and is further tested using RCM data. We consider months and subregions of Europe separately, and find a seasonality in the temperature dependence of precipitation intensity, with a general increase in winter and a decrease in summer. Furthermore, we identify regional characteristics of the temperature dependence with relatively strong positive increases in the northeast of Europe in winter, and weaker wintertime response in the southwest.

[31] Using model data, we draw a connection between daily averaged atmospheric water vapor, cloud water and precipitation intensity. From this analysis we find that moisture availability rather than the moisture storage capacity of the atmosphere is the bottleneck when considering precipitation intensity during the warm season. Conversely, in winter we find the C-C equation to indeed control the upper limit of precipitation intensity. We conclude that this connection should be explored further on a subdaily scale, for which the true precipitation intensity is better represented and the results are not dominated by P_{ls} in the same way.

[32] Furthermore, we find a different relationship between precipitation intensity and temperature for model simulated P_{ls} and P_c. While in winter the large-scale contribution clearly dominates on the daily timescale, the percentiles are equally influenced by convective precipitation at the higher end of the temperature range in summer. This leads to a more elaborate temperature dependence of precipitation intensity in the warm season, for which we find negative dependence which are interrupted by a brief positive dependence at around ten to twenty degrees Celsius. The main behavior can be explained by the decreasing trend of P_{ls}, due to a lack of saturation at a larger scale. For P_c we find a peak intensity at a certain temperature. This temperature varies with seasons, but not with latitude. We argue that this temperature is dependent on the process leading to the convective precipitation itself, rather than being related to the mean temperature of the region studied.

[33] The temperature dependence of precipitation intensity as a whole is a superposition of the relative contribution of the large-scale and convective precipitation types. P_{ls} clearly dominates throughout winter. This is due to the southward intrusion of moist Atlantic and Arctic as well as northward propagation of Mediterranean air masses. We find the intensity of precipitation to be linked to the amount of moist static energy carried by these systems. The cool land air has a low moisture holding capacity, and is readily saturated by the advected moisture. Therefore we can expect the C-C relation to describe the change in precipitation intensity in this season. However, in the warmer summer, the atmosphere has a much higher moisture holding capacity, and is therefore not as readily saturated. At the same time, the supply of moisture may be lower due to the more local character of moisture transport in that season. A drying out of the soil in summer may also lead to higher temperatures, meaning that the causal relationship is reversed in comparison to the winter months [*Trenberth and Shea*, 2005].

[34] A further analysis underway at the Max Planck Institute for Meteorology (C. Moseley, personal communication, 2009) is concerned with atmospheric moisture fluxes. Generally, the European domain benefits from moisture convergence (net influx greater than zero) in winter, while relatively neutral convergence characterizes the summer season. This leads to a more localized nature of precipitation formation (recycling processes) in that part of the year.

[35] In the light of a changing climate, often defined as a change in mean surface temperature, our study motivates further investigations: Does the relation between precipitation intensity and temperature change in a future climate? This questions could be approached by analyzing scenario simulations, such as those produced for the ENSEMBLES project [*Hewitt and Griggs*, 2004]. In the case of similar future statistical relationships as those presented here, our results would mean that in a warmer climate in winter more intense daily precipitation events can be expected in Europe, while summer events would generally become weaker. These questions are the topic of a future study.

[36] To build further upon the present study, a higher temporal resolution would be desirable, such that the convective precipitation can be distinguished more easily in the observational data. It would also be interesting to expand this study to include global data. This would open up the possibility to test the results found here in different climates, and thereby test the generality of the findings.

[37] **Acknowledgments.** This study was partly funded by the European Union FP6 project WATCH (contract 036946). We acknowledge the model data sets from the REMO, HIRHAM, and HadRM groups and the gridded data set from the EU-FP6 project ENSEMBLES (http://www.ensembles-eu.org) and the data providers in the ECA&D project (http://eca.knmi.nl). Thanks to A. Haensler for useful comments.

References

Allen, M. R., and W. J. Ingram (2002), Constraints on future changes in climate and the hydrologic cycle, *Nature*, *419*, 224–232.

Boberg, F., P. Berg, P. Thejll, W. J. Gutowski, and J. H. Christensen (2008), Improved confidence in climate change projections of precipitation evaluated using daily statistics from the PRUDENCE ensemble, *Clim. Dyn.*, *32*, 1097–1106, doi:10.1007/s00382-008-0446-y.

Christensen, J. H., and O. B. Christensen (2007), A summary of the PRUDENCE model projections of changes in European climate by the end of this century, *Clim. Change*, *81*, 7–30, doi:10.1007/s10584-006-9210-7.

Christensen, J. H., O. B. Christensen, P. Lopez, E. van Meijgaard, and M. Botzet (1996), The HIRHAM4 regional climate model, *DMI Internal Rep. 96-4*, Danish Meteorological Institute, Copenhagen, Denmark.

Collins, M., B. B. B. Booth, G. R. Harris, J. M. Murphy, M. H. Sexton, and M. J. Webb (2006), Towards quantifying uncertainty in transient climate change, *Clim. Dyn.*, *27*(2–3), 127–147.

Dai, A. (2006), Precipitation characteristics in eighteen coupled climate models, *J. Clim.*, *19*, 4605–4630.

Efron, B., and R. J. Tibshirani (1993), *An Introduction to the Bootstrap*, Chapman & Hall, New York.

Emori, S., and S. J. Brown (2005), Dynamic and thermodynamic changes in mean and extreme precipitation under changed climate, *Geophys. Res. Lett.*, *32*, L17706, doi:10.1029/2005GL023272.

Gregory, D. (1995), A consistent treatment of the evaporation of rain and snow for use in large-scale models, *Mon. Weather Rev.*, *123*, 2716–2732.

Gregory, D., and S. Allen (1991), The effect of convective scale downdrafts upon nwp and climate simulations, in *Ninth Conf. Numerical Weather Prediction*, Am. Meteorol. Soc., Denver, Colorado, pp. 122–123.

Gregory, D., and P. Rowntree (1990), A mass-flux convection scheme with representation of cloud ensemble characteristics and stability dependent closure, *Mon. Weather Rev.*, *118*, 1483–1506.

Groisman, P. Y., R. W. Knight, D. R. Easterling, T. R. Karl, G. C. Hegerl, and V. N. Razuvaev (2005), Trends in precipitation in the climate record, *J. Clim.*, *18*, 1326–1350.

Gutowski, W. J., K. A. Kozak, R. W. Arritt, J. H. Christensen, J. C. Patton, and E. S. Takle (2007), A possible constraint on regional precipitation intensity changes under global warming, *J. Hydrometeorol.*, *8*, 1382–1396, doi:10.1175/2007JHM817.1.

Haerter, J. O., and P. Berg (2009), Unexpected rise in extreme precipitation due to shift in rain type?, *Nat. Geosci.*, *2*, 372–373.

Haylock, M. R., N. Hofstra, A. M. G. K. Tank, E. Klok, P. D. Jones, and M. New (2008), A European daily high-resolution gridded dataset of surface temperature and precipitation, *J. Geophys. Res.*, *113*, D20119, doi:10.1029/2008JD010201.

Hennessy, K. J., J. M. Gregory, and J. F. B. Mitchell (1997), Changes in daily precipitation under enhanced greenhouse conditions, *Clim. Dyn.*, *13*, 667–680.

Hewitt, C. D., and D. J. Griggs (2004), Ensembles-based predictions of climate changes and their impacts, *Eos Trans. AGU*, *85*, 566, doi:10.1029/2004EO520005.

IPCC Fourth Assessment Report (2007), Observations: Surface and Atmospheric Climate Change, in *Climate Change 2007: The Physical Science*

Basis. Contribution of Working Group I to the Fourth Assessment Report of the Intergovernmental Panel on Climate Change, edited by S. Solomon, Cambridge Univ. Press, Cambridge, U. K.

Jacob, D., et al. (2001), A comprehensive model intercomparison study investigating the water budget during the baltex-pidcap period, *Meteorol. Atmos. Phys.*, *77*, 19–43.

Landsberg, H. E. (1970), *Climates of Northern and Western Europe*, vol. 5, Elsevier, Amsterdam, Netherlands.

Lenderink, G., and E. van Meijgaard (2008), Increase in hourly precipitation extremes beyond expectations from temperature changes, *Nat. Geosci.*, *1*, 511–514.

Lohmann, U., and E. Roeckner (1996), Design and performance of a new cloud microphysics scheme developed for the echam4 general circulation model, *Clim. Dyn.*, *12*, 557–572.

Meehl, G. A., F. Zwiers, J. Evans, T. Knutson, L. Mearns, and P. Whetton (1999), Trends in extreme weather and climate events: Issues related to modeling extremes in projections of future climate change, *Bull. Am. Meteorol. Soc.*, *81*(3), 427–436.

Meehl, G. A., J. M. Arblaster, and C. Tebaldi (2005), Understanding future patterns of increased precipitation intensity in climate model simulations, *Geophys. Res. Lett.*, *32*, L18719, doi:10.1029/2005GL023680.

Nordeng, T. (1994), Extended versions of the convective parameterization scheme at ecmwf and their impact on the mean and transient activity of the model in the tropics, *Tech. Memo. 206*, European Centre for Medium-Range Weather Forecasts, Reading, U. K.

Semenov, V. A., and L. Bengtsson (2002), Secular trends in daily precipitation characteristics: Greenhouse gas simulation with a coupled AOGCM, *Clim. Dyn.*, *19*, 123–140.

Senior, C., and J. Mitchell (1993), CO_2 and climate: The impact of cloud parameterization, *J. Clim.*, *6*, 393–418.

Sun, Y., S. Solomon, A. Dai, and R. W. Portmann (2007), How often will it rain?, *J. Clim.*, *20*, 4801–4818, doi:10.1175/JCLI4263.1.

Tank, A. M. G. K., et al. (2002), Daily dataset of 20th-century surface air temperature and precipitation series for the european climate assessment, *Int. J. Climatol.*, *22*, 1441–1453.

Tiedtke, M. (1989), A comprehensive mass flux scheme for cumulus parameterization in large-scale models, *Mon. Weather Rev.*, *117*, 1779–1800.

Tompkins, A. (2002), A prognostic parameterization for the subgrid-scale variability of water vapor and clouds in large-scale models and its use to diagnose cloud cover, *Atmos. Sci.*, *59*, 1917–1942.

Trenberth, K. E., and D. J. Shea (2005), Relationships between precipitation and surface temperature, *Geophys. Res. Lett.*, *32*, L14703, doi:10.1029/2005GL022760.

Trenberth, K. E., A. Dai, R. M. Rasmussen, and D. B. Parsons (2003), The changing character of precipitation, *Bull. Am. Meteorol. Soc.*, *84*, 1205–1217.

Trenberth, K., J. Fasullo, and L. Smith (2005), Trends and variability in column-integrated atmospheric water vapor, *J. Clim. Dyn.*, *24*, 741–758.

P. Berg, Water Cycle and Climate Modeling, Institute for Meteorology and Climate Research, University of Karlsruhe and Karlsruhe Forschungszentrum, Karlsruhe, Germany. (peter. berg@imk.fzk.de)

J. H. Christensen and P. Thejll, Danish Climate Centre, Danish Meteorological Institute, Lyngbyvej 100, DK-2100 Copenhagen, Denmark.

J. O. Haerter and S. Hagemann, Land in the Earth-System, Max Planck Institute for Meteorology, Bundesstr. 53, D-20146 Hamburg, Germany.

C. Piani, International Center for Theoretical Physics, Strada Costiera 11, I-34014 Trieste, Italy.